USP4 is regulated by Akt phosphorylation and deubiquitylates TGF-β type I receptor

Long Zhang,^{*1} FangFang Zhou,^{*1¶} Yvette Drabsch,¹ Ewa Snaar-Jagalska², Craig

Mickanin³, Huizhe Huang⁴, Kelly-Ann Sheppard³, Chris Lu³ and Peter ten Dijke^{1¶}

¹Department of Molecular Cell Biology, Leiden University Medical Center, Postbus 9600 2300 RC Leiden, The Netherlands.

²Institute of Biology, Leiden University, The Netherlands.

³Novartis Institutes for Biomedical Research, 250 Massachusetts Avenue, Cambridge, Massachusetts 02139, USA.

³Faculty of Basic Medical Sciences, Chonqing Medical University, Medical College Road 1, 400016 Chongqing China.

*Those authors contribute equally to this work.

[¶]Correspondence: Department of Molecular Cell Biology, Leiden University Medical Center, Postbus 9600, 2300 RC Leiden, The Netherlands E-mail: <u>p.ten_dijke@lumc.nl</u> (ten Dijke P); <u>F.zhou@lumc.nl</u> (F.zhou); Phone: +31 71 526 9200; Fax: + 31 71 526 8270

Stability and membrane localization of Transforming growth factor- β (TGF- β) type I receptor (TBRI) is essential for controlling TGF-B signaling^{1,2}. TBRI is targeted for ubiquitination-mediated degradation by Smad7/Smurf2 complex. However, it is unclear whether polyubiquitin modified TBRI can be reversed. Here we performed a genome-wide gain of function screen and identified ubiquitin-specific protease (USP) 4 as a strong inducer of TGF-B signaling. Putative oncogenic USP4 was found to interact with TBRI as deubiquitinating enzyme thus maintains TBR1 levels at the plasma membrane. Depletion of USP4 mitigates TGF-β-induced breast cancer cell migration, epithelial to mesenchymal transition and metastasis. Importantly, Akt/Protein kinase B (PKB)^{3,4}, which has been associated with poor prognosis in breast cancer ^{5, 6}, associates with and phosphorylates USP4. Akt mediated phosphorylation relocates USP4 to cytoplasm and membrane and is required for maintaining its protein stability. Moreover, Akt-induced breast cancer cell migration was inhibited by USP4 depletion and TBRI kinase inhibition. Our results identified USP4 as an important determinant for crosstalk between TGF-B and Akt, which provides new opportunities for cancer treatment.

TGF-β is of critical importance for embryogenesis and tissue homeostasis of multicellular organisms. Perturbations in its signaling pathways have been linked to a diverse set of human diseases, including cancer^{7, 8}. The TGF-β activated serine/threonine kinase receptor complex propagates the signal by phosphorylating receptor regulated (R)-Smads, i.e Smad2 and Smad3. Activated R-Smads form hetero-oligomers with Smad4 that accumulate into the nucleus to regulate a large number of target genes ^{1, 2, 7, 8}. Besides Smad pathway, also non-Smad signaling pathways are initiated that include the phosphatidylinositol-3-kinase (PI3K)/AKT pathway⁹⁻¹¹. These non-canonical pathways are also activated by growth factors that signal via tyrosine kinase receptors to mediate cell proliferation, survival and migration. During cancer progression, TGF-β frequently switches from tumor suppressor to tumor promoter. Oncogenic signals may blunt TGF-β-induced growth arrest and apoptosis, while enhance TGF-β-induced pro-invasive and pro-metastatic responses, and this may involve a change in balance between canonical and non-Smad signaling¹²⁻¹⁴

TGF-β signaling is intricately controlled by multiple positive and negative regulators. Smad7 is a potent negative regulator of TGF-β signaling by recruiting Smurf E3 ubiquitin ligases to the activated TβRI and targeting this receptor for degradation ^{15, 16}. Whether this process can be reversed via action of specific deubiquitinating enzymes (DUBs)¹⁷⁻²⁰ is unknown. To identify novel critical components of TGF-β signaling, we performed a gain of function screen overexpressing 27,000 genes using a TGF-β-induced Smad3/4 driven transcriptional reporter as read out. Multiple DUBs, including USP4, -11 -19 and -15 potently activated the TGF-β-induced signal (Fig. 1a), of which USP15 was just known as a deubiquitinating enzyme for R-Smad²¹. An independent screen with 69 Flag-tagged DUB cDNAs (with comparable expression levels of each DUB) confirmed the same USPs as selective activators of TGF- β , but not IL1 β /NF κ -induced transcriptional response (Supplementary Fig. S1a and S1b and data not shown). In contrast to USP4 wild-type, the USP4 CS mutant (carrying a point mutation in one of the key cysteines of the catalytic domain) did not potentiate TGF- β signaling (Fig.1b). This suggests that the DUB activity is needed for this response. Knock-down with two independent shRNAs that selectively target USP4, demonstrated that endogenous USP4 expression is required for maximal TGF-B-induced transcriptional response in HEK293T cells (Fig. 1c). These results were consolidated in other cell types. Ectopic expression of wild-type USP4, but not the CS mutant increased both magnitude and duration of TGF- β induced Smad2/Smad4 complex formation in MCF10A-Ras (M2) breast cancer cells (Fig. 1d). Depletion of endogenous USP4 decreased this effect in MDA-MB-231 breast cancer cells (Fig.1e). Moreover, both duration and intensity of TGF-B-induced Smad2 phosphorylation and downstream target gene expression were impaired in USP^{-/-} cells compared to USP^{+/+} mouse embryonic fibroblasts (MEFs) (Fig. 1f and 1g). To investigate the role of USP4 in vivo we depleted USP4 in zebrafish using morpholino oligonucleotides (with depleting effects confirmed, data not shown), and observed a serious epiboly defect before the formation of zebrafish tail bud is completed (data not show). Usp4 morphant embryos showed severe inhibition in expression of TGF-β targets goosecoid (gsc) and notail (ntl) (Fig. 1h), and these genes were elevated in embryos injected with *usp4* mRNA as measured by *in situ* hybridization (Fig. 1h). Consistently, qPCR results of gsc, ntl, sox17 and sox32 confirmed the effects of USP4 expression on

target gene expression *in vivo* (Fig. 1i), Taken together, these results indicate that USP4 is a critical regulator of TGF- β signaling in mammalian cells and zebrafish embryos.

The results above indicate that USP4 acts as a deubiquitylase in the TGF-β pathway, and operates upstream of R-Smad activation. This prompted us to test whether USP4 targets TGF-β receptor function. We first analyzed whether USP4 and TβRI can physically interact with each other. Upon overexpression, USP4 binds TβRI (Supplementary Fig S2a). Interestingly, the association with (endogenous) USP4 was more efficient upon TβRI activation (Supplementary Fig S2a and S2b). Moreover, USP4 antibodies were able to co-immunoprecipate ¹²⁵I-TGF-β affinity labeled endogenous receptors, which validates the interaction between USP4 and TGF-β receptor (Fig. 2a). Furthermore, endogenous USP4 was found to interact with TβRI in a TGF-β-induced manner in HeLa cells (Fig. 2b). Therefore, USP4 binds TβRI at physiological conditions.

We eluted TβRI from a USP4 complex. We found wild-type USP4 associated TβRI was not ubiquitinated while USP4 cs mutant associated TβRI was highly ubiquitinated (Fig. S2c). We thus asked if USP4 serves as a DUB for TβRI. Firstly, Flagtagged caTβRI proteins were affinity purified and their ubiquitination pattern was visualized by immunoblotting for HA–ubiquitin; polyubiquitination appeared as a major modification of TβRI. Overexpression of wild-type USP4, but not of a catalytically inactive USP4 mutant, inhibited TβRI Lysine 48 polyubiquitination in the absence or presence of proteasome inhibitor MG132 (Fig. 1c). TGF-β receptor signaling induces Smad7 expression, which subsequently targets TβRI degradation by recruiting E3 ligase Smurf2 ^{15, 16}. USP4 opposed Smad7/Smurf2-induced TβRI ubiquitination (Supplementary Fig. 2d), and blocked TGF-β-induced TβRI ubiquitination at the endogenous level (Fig. 2d). Conversely, USP4 depletion enhanced TGF-β-induced TβRI Lysine 48 polyubiquitination (Fig.2e). The modification of TβRI by Lysine-48 linked polyubiquitination has been reported to promote its internalization and degradation²². We therefore tested whether USP4 misexpression can regulate TβRI levels at the plasmembrane, the location where signaling is initiated ²². When coexpressed with wild-type USP4, but not with the catalytically inactive mutant, biotin-labeled cell surface TβRI receptor displayed a prolonged half-life (Fig. 2f). In line with this finding, USP4 depletion in MDA-MB-231 cells led to lower cell surface TβRI expression and accelerated degradation (Fig 2g). Moreover, when compared to USP4^{+/+} MEFs, USP4^{-/-} MEFs showed lower expression level and shorter half-life of TβRI (Fig.2h). These findings indicate that USP4 is a DUB for TβRI and contributes to increased stability of TβRI at the plasmamembrane.

USP4 is highly expressed in different cancers, including breast cancer ²³. TGF-β stimulates epithelial to mesenchymal transition (EMT), cell migration, invasion and metastasis of breast cancer^{7, 24}. Typical EMT changes are: upregulation of N-cadherin, fibronectin, smooth muscle actin and vimentin and downregulation of E-cadherin ²⁵. Upon depletion of USP4, TGF-β-induced changes in EMT marker expression were attenuated (Fig. 3a). Conversely, ectopic expression of USP4, but not its CS inactive mutant, potentiated these TGF-β-induced changes in expression (Fig.3b). Consistent with these results, USP4 knockdown attenuated TGF-β-induced migration of MDA-MB-231 cells (Fig. 3c). These results suggest that USP4 regulates TGF-β-induced EMT and migration of breast cancer cells *in vitro*.

We next examined the effect of USP4 misexpression in breast cancer cells in vivo by using zebrafish embryo xenograft model where mammalian tumor cells are injected into the zebrafish embryonic blood circulation (for technical details, see materials and methods) (Fig. 3d). MCF10A-Ras cells stably infected with wild-type USP4, inactive USP4 CS mutant or an empty vector control were injected into the blood circulation of the zebrafish embryo. Invasion and micrometastasis were measured using fluorescent microscopy every second day in the avascular tail fin area of the embryo. Confocal microscopy was used to visualize the invading tumor cells (labeled in red), against the Fli:GFP background of the zebrafish embryo which labels blood vasculature (green). Individual cell invasion can be detected in this model (He et al submitted). Over 5 days, a marked increase of invasion was visible upon ectopic expression of wild type USP4, but not its inactive CS mutant (Fig. 3e, f). Treatment with SB431542, a selective TβRI kinase inhibitor, reduced the invasion and micrometastasis of all samples (Fig.3f and 3g). At the end of the 5 days, wild-type USP4 infection in MCF10A-Ras cells resulted in 55% of zebrafish embryos displaying invasion, whilst the USP4 cs mutant and control samples showed invasion in 35% and 36% embryos, respectively (p < 0.01) (Fig. 3f and 3g). Due to the transparent nature of the zebrafish embryo, invading cells were also visible with light microscopy (Fig.3h).

MDA-MB-231 is a highly aggressive human breast cancer cell line, and metastasis of these cells in a mouse and zebrafish embryo xenograft model were found to be dependent on TGF- β receptor signaling in tumor cells ^{26, 27} (Drabsch and ten Dijke, unpublished results). In vitro qPCR analysis indicated that endogenous USP4 is required for efficient induction of metastasis-related TGF- β target genes, such as *IL-11, CTGF*,

7

CXCR4, PTHrP and *MMPs* (Fig. 3i). Similar results were obtained with other shUSP4 lentivirus (data not shown).

Subsequently, invasion and metastasis properties of USP4 depleted MDA-MB-231 cells were analyzed in zebrafish embryos. MDA-MB-231 cells with stable depletion of endogenous USP4 were injected into the ducts of Cuvier 48 hpf. The zebrafish embryos were analyzed over 5 dpi (see representative images of the tail fin area in Fig. 3j). The control cells showed 62% of zebrafish embryos with invasion, whereas knockdown of USP4 by 3 independent shRNAs attenuated the invasion (Fig. 3k). Furthermore, the amount of micrometastasis was also reduced upon USP4 depletion (Fig.3l). Taken together, these results suggest that USP4 stimulates TGF-β-induced breast cancer invasion and metastasis.

When we analyzed the subcellular distribution of endogenous USP4, we found it to be mainly present in nucleus. This prompted us to investigate how USP4 could maintain cell surface TβRI levels at the plasmamembrane. Sequence analysis revealed that USP4 contains an Akt consensus RxRxxS/T phosphorylation motif ⁶ at Ser 445. The motif is also conserved in USP4 orthologues (Fig 4a). It has been shown that for certain Akt substrates, phosphorylation triggers their nuclear export ²⁸. We therefore reasoned that USP4 is a substrate of Akt, whose phosphorylation may influence USP4 subcellular localization. Consistent with the hypothesis, we found that an activated allele of Akt (myr-Akt1) interacts with USP4 in transfected cells (Fig. 4b). In addition, USP4 was found to associate with Akt endogenously (Fig. 4c). To examine whether USP4 is a substrate for Akt, we used a phospho-specific antibody that recognizes the optimal Akt consensus phosphorylation motif (p-Ark substrate). We found that expression of

Nature Precedings : hdl:10101/npre.2012.6804.1 : Posted 19 Jan 2012

activated Akt significantly enhanced the phosphorylation of wild-type USP4, whereas USP4-S445A phosphorylation was not detected by p-Artk substrate antibody (Fig. 4b and 4d). The reactivity of USP4 with this antibody was reversed when the cell lysates were incubated with lambda phosphatase (Fig. 4e). Moreover, insulin growth factor (IGF)-1 or TGF-β-induced endogenous USP4 phosphorylation as detected by the Akt substrate antibody. Notably, the phosphorylation of USP4 was decreased in cells that were treated with LY294002, a selective inhibitor for phosphatidylinositol 3-kinase (PI3K) (Fig. 4f).

To investigate the effect of Akt on USP4 subcelluar localization we used HeLa cells stably expressing wild type USP4 or USP4 S44A/S445D mutants and confocal analysis. While USP4 S445A mutant was almost exclusively present in the nuclei, the USP4 S445D showed a significant increase in cytoplasmic localization when compared with wild-type USP4 (Fig. 4g). Importantly, LY294002 treatment reduced the cytoplasmic signal of endogenous USP4 (Fig. 4h). To validate these findings, we examined the effect of activated myr-Akt on the localization of wild type USP4 or S44A/S44D USP4 mutants using immunofluorescence microscopy and cellular fractionation. We observed that the expression of activated myr-Akt promoted the cytoplasmic and membrane localization of wild-type USP4 (Fig 4i and 4j). In contrast, in the presence of activated Akt the non-phosphorylatable S445A USP4 mutant was still restricted to the nuclear compartment (Fig 4i and 4j). Conversely, a significant fraction of the phospho-mimetic USP4 S445D mutant was located in the cytoplasm, and its localization was not much affected by the expression of activated Akt (Fig 4i and data not shown). Futhermore, endogenous USP4 located in membrane and cytoplasm became completely nuclear or increased in membrane/cytoplasm localization upon LY294002

treatment and activated Akt expression, respectively (Fig. 4k). These results together indicate that Akt-induced USP4 phosphorylation affects its subcelluar distribution by promoting more USP4 to be present in membrane and cyoplasm.

USP4 is a stable protein as it can deubiquitylate itself²⁹; Consistent with this, wild type USP4 was found to be more stable than USP4 CS mutant (data not shown). Time-course experiments in cells subjected to treatment with protein synthesis inhibitor cycloheximide (CHX) in the absence or presence of LY294002 or ectopically expressed activated Akt revealed that USP4 halflife was shortened and prolonged, respectively (Fig 5a). Consistent with these results we found that the S445A mutant was degraded more rapidly than wild-type USP4 and S445D mutant (Fig. 5b). Compared with wild-type USP4, S445A mutant demonstrated an increased level of conjugation with polyubiquitin chains (Fig. 5c), suggesting that the impaired protein halflife of the S445A mutant is due to its elevated ubiquitination. We found that USP4 formed complex with itself and also interacted with USP15, USP19 and USP11, the other DUBs that were identified in our genetic screen (Fig. S3a). Mutation of the Akt phosphorylation site on USP4 (S445A mutant) mitigated the ability to associate with itself or other USPs (Fig. 5d and 5e, Supplementary Fig. S3b). Particularly, when USP4 was coexpressed with USP15, we observed an elevation in USP4 expression (Supplementary Fig. S3a). An enforced long stability of USP4 protein was detected when it was co-expressed with USP15 (Fig. 5f). These data suggest that Akt mediated phosphorylation on Ser 445 is required for USP4 to form homometric complexes and heterometric complexes with other DUBs, particularly with USP15. As USP4 binding partners, USP15, USP19 and USP11 were also observed to deubiquitinate TβRI when they were overexpressed (Fig.S3c). We focused on USP15

10

and found it could also serve as a deubiquitylase for T β RI (Supplementary Fig. S3d) but that this relied on endogenous USP4 (Supplementary Fig. S3e).

Consistent with the notion that wild-type USP4 and USP4 S445D mutant are more located at plasmamembran and stable than USP4 S445A mutant, we found that S445A mutant had lost the ability to remove polyubiquitin chains from T β RI (Fig. 5g). This suggests that Akt mediated USP4 phosphorylation is required for USP4 to serve as a deubiquitylase for TBRI. To further investigate the functional cooperation between PI3K/Akt and TGF- β /T β RI signaling pathways via USP4, we examined the effect of USP4 depletion or TBRI kinase inhibitor on IGF-1- or activated myr-Akt-induced migration of MDA-MB -231 cells. We found that both treatments could partially reduce IGF-1/Myr-Akt-induced cell migration (Fig. 5h and 5i). Our current study suggest a working model in which in invasive/metastatic breast cancer cells, Akt activated by growth factors/TGF-B induces phosphorylation of USP4, which associates with TBRI in the membrane to stabilize it, and then enforces the TGF-B receptor-induced promigratory/invasive and metastatic responses in breast cancer cells (Fig. 5j). Akt has been shown to reduce Smad3 function in Hep3B cells in which TGF-β induces an apoptotic response ^{30, 31}. Akt can directly associate with unphosphorylated Smad3 and sequester it outside the nucleus. However, Smad3 levels are often reduced in advanced human tumors with low levels being sufficient for tumor promotion^{32, 33}. Activation of Akt may redirect TGF- β signaling and thereby contribute to its switch from tumor suppressor to tumor promoter. With DUBs being druggable targets³⁴, it would be interesting to develop inhibitors for USP4 and test their potential for anti-invasive and anti-metastatic properties.

Nature Precedings : hdl:10101/npre.2012.6804.1 : Posted 19 Jan 2012

11

METHODS

Cell culture and reagents. MEFs from wild-type and USP4^{-/-} mice were kindly provided by Xiongbin Lu (University of Texas MD Anderson Cancer Center, Houston, TX, USA)³⁵. HEK293T cells, HeLa cervical cancer cells, MDA-MB-231breast cancer cells and MEFs were cultured in Dulbecco's modified Eagle's (DMEM) with 10% FBS and 100 U/ml penicillin/streptomycin. Myc-USP4 wt and Myc-USP4 C311S expression constructs were cloned and verified by DNA sequencing. USP4 wt and C311S mutant were subcloned into pLV bc puro lenti virus construct. USP4 S445A and USP4 S445D were made by side directed mutation and confirmed by sequencing. Myr-Akt constructs were kindly provided by Dr. Paul Coffer. MG132 were purchased from Sigma; IGF-1(R&D 291-G1), LY294002 (Cell signaling), λ-phosphatase (Biolabs). The antibodies used for immunoprecipitation, immunoblotting and immunofluorescence were raised against the following proteins: β-actin (A5441, Sigma), c-Myc (a-14, sc-789, Santa Cruz biotechnology), HA (Y-11, sc-805, Santa Cruz biotechnology), HA (12CA5), Flag (M2, Sigma), USP4 (U0635, Sigma), TBRI (V22, Santa Cruz), Akt (#2938 Cell signaling), phosphor-Akt substrate (RXRXXS*/T*) (#10001, Cell Signaling), phosphor-Akt (Ser473) (#9271, Cell Signaling), V5 (Invitrogen), USP15 (BETHYL), USP11 (BETHYL A301-613A), USP19 (BETHYL A301-586A), N-cadherin(610920 BD), Tubulin (#2146 Cell signaling), HDAC3 (#3949 Cell signaling), Smad4 (B8 Santa Cruz), Smad2/3 (610842 BD), phospho-Smad2 (#3101 Cell signaling), Lys48-polyUb (#8081 Cell signaling), Ub (P4D1 Santa Cruz), Fibronectin (Sigma), SMA(Sigma), vimentin (#5741 Cell signaling), E-cadherin (BD 610181), HA (12CA5).

Lentiviral transduction and generation of stable cell lines. Lentiviruses were produced by transfecting shRNA targeting plasmids together with helper plasmids pCMV-VSVG, pMDLg-RRE (gag/pol), and pRSV-REV into HEK293T cells. Cell supernatants were harvested 48 h after transfection and were either used to infect cells or stored at -80 °C. To obtain stable cell lines, cells were infected at low confluence (20%) for 24 h with lentiviral supernatants diluted 1:1 with normal culture medium in the presence of 5 ng/ml of polybrene (Sigma). 48 h after infection, cells were placed under puromycin selection for one week, and then passaged before use. Puromycin was used at 1 μ g/ml to maintain MDA-MB-231 cells. Lentiviral shRNAs were obtained from Sigma (MISSION® shRNA). Typically, 5 shRNAs were identified, tested, and the most effective two shRNAs were used for the experiment. We used TRCN0000004040 (#1), TRCN0000004041 (#2) and TRCN000004042 (#3) for human USP4 knockdown.

Transcription reporter assay. HEK293T cells were seeded in a 24-well plate and transfected with the indicated plasmids using calcium phosphate. 24 h after transfection, cells were treated with TGF- β 3 (5 ng/ml) overnight or left untreated and then harvested. Luciferase activity was measured with a Perkin Elmer luminometer. The internal transfection control, β -gal (30 ng), was used to normalize luciferase activity. Each experiment was performed in triplicate and the data represent the mean \pm SD of three independent experiments.

Immunoprecipitation, immunoblotting and biotinylation. Cells were lysed with 1 ml lysis buffer (20 mM Tris-HCl pH 7.4, 2 mM EDTA, 25 mM NaF, and 1% Triton X-100)

plus protease inhibitors (Sigma) for 10 min at 4°C. After centrifugation at $12 \times 10^3 \times g$ for 15 min, the protein concentration was measured and equal amounts of lysate used for immunoprecipitation. Immunoprecipitation was performed with different antibodies and protein A-sepharose (GE Healthcare Bio-Sciences AB) for 3 h at 4°C. Thereafter, the precipitants were washed three times with washing buffer (50 mM Tris-HCl pH 8.0, 150 mM NaCl, 1% Nonidet P-40, 0.5% sodium deoxycholate, and 0.1% SDS) and the immune complexes eluted with sample buffer containing 1% SDS for 5 min at 95°C. The immunoprecipitated proteins were then separated by SDS-PAGE. Western blotting was performed with specific antibodies and secondary anti-mouse or anti-rabbit antibodies conjugated to horseradish peroxidase (Amersham Biosciences). Visualization was achieved with chemiluminescence. For proteins that close to IgG heavy chain, for instance TBRI blottings, protein A-HRP was used. For biotinylation analysis of cell surface receptors, the cells were biotinylated for 40 min at 4°C and then incubated at 37°C for indicated times. The biotinylated cell surface receptors were precipitated with strepavidin beads and analyzed by immunoblotting.

Immunofluorescence. Cells were fixed for 10 min in 4% paraformaldehyde in phosphate buffered saline (PBS), permeabilized with 0.2% TritonX100-PBS, and then blocked with 3% bovine serum albumin (BSA) in PBS for 30 min at room temperature. Specific first antibodies were diluted in 3% BSA-PBS and incubated with the slides for 3 h at room temperature. Secondary AlexaFluor488-labeled anti-mouse antibody (Molecular Probes) or AlexaFluor593-labeled anti-rabbit antibody (Molecular Probes) were added at a dilution of 1:200 in 3% BSA-PBS and incubated for 1 h at room temperature. Coverslips

were mounted with VECTASHIELD mounting medium (Vector Laboratories, Inc.). Fluorescence images were acquired with a Zeiss Axioplan microscope.

Ubiquitination assay. Cells were washed with PBS and lysed in two pellet volumes of RIPA buffer (20 mM NAP pH 7.4, 150 mM NaCl, 1% Triton, 0.5% sodium-deoxycholate, and 1% SDS) supplemented with protease inhibitors and 10 mM N-ethylmaleimide (NEM). Lysates were sonicated, boiled at 95°C for 5 min, diluted with RIPA buffer containing 0.1% SDS, then centrifuged at 4°C (16 x 10^3 x g for 15 min). The supernatant was incubated with specific antibody and protein A-sepharose for 3 h at 4°C. After extensive washing, bound proteins were eluted with 2 x SDS sample buffer and separated by SDS-PAGE, followed by immunoblotting.

Nickel pull down assay. Cells were lysed in 6M guanidine-HCl, 0.1 M Na₂HPO₄/NaH₂PO₄, and 10 mM imidazole, followed by nickel bead purification and immunoblot analysis.

Real-time RT-PCR (qRT-PCR). Total RNAs were prepared using NucleoSpin® RNA II kit (BIOKÉ, Netherlands). 1 µg RNA was reverse-transcribed using the RevertAid[™] First Strand cDNA Synthesis Kits (Fermentas). Real-time PCR was conducted with SYBR Green incorporation (Applied Bioscience) using a StepOne Plus real-time PCR system (Applied Bioscience). All of the values of the target gene expression level were normalized to GAPDH. All Primers used for qRT-PCR are listed as follows:

CTGF forward, 5'-TGCGAAGCTGACCTGGAAGAGAA-3'

CTGF reverse, 5'-AGCTCGGTATGTCTTCATGCTGGT-3' IL-11 forward, 5'-ACTGCTGCTGCTGAAGACTC-3' IL-11 reverse, 5'-CCACCCCTGCTCCTGAAATA-3' CXCR4 forward, 5'-CAGTGGCCGACCTCCTCT-3' CXCR4 reverse, 5'-CAGTTTGCCACGGCATCA-3' PTHrP forward, 5'-TTCTTCCCAGGTGTCTTGAG-3' PTHrP reverse, 5'-TTTACGGCGACGATTCTTCC-3' MMP2 forward, 5'-TGCCTGGAATGCCAT-3' MMP2 reverse, 5'-GTTCTCCAGCTTCAGGTAAT-3' MMP9 forward, 5'-TACTGTGCCTTTGAGTCCG-3' MMP9 reverse, 5'-TTGTCGGCGATAAGGAAG-3' GAPDH forward, 5'-CCATCCACAGTCTTCTGGGT-3' GAPDH reverse, 5'-GATCATCAGCAATGCCTCCT-3' mCxcr4 forward, 5'-TTACCCCGATAGCCTGTGGAT-3' mCxcr4 reverse, 5'-GCAGGACGAGACCCACCAT-3' mSmad7 forward, 5'-TGGATGGCGTGTGGGTTTA-3' mSmad7 reverse, 5'-TGGCGGACTTGATGAAGATG-3' mSnoN forward, 5'-AAGCAAGCGTGATTCAGAAGATT-3' mSnoN reverse, 5'-CCCCTTGTCGTCTTCACCAT-3' mCTGF reverse, 5'-GGCCTCTTCTGCGATTTCG-3' mCTGF forward, 5'-CCATCTTTGGCAGTGCACACT-3' mPAI-1 forward, 5'- GCCAACAAGAGCCAATCACA-3' mPAI-1 reverse, 5'- AGGCAAGCAAGGGCTGAAG-3'

mGAPDH forward, 5'-AACTTTGGCATTGTGGAAGG-3' mGAPDH reverse, 5'-ACACATTGGGGGGTAGGAACA-3'

Zebrafish embryo assay. Zebrafish (*Danio rerio*), AB strain, were kept at 28.5°C under a light and dark cycle of 14 and 10 hours, respectively. Fish staging and embryo production were carried out as described previously^{36, 37}. Capped mRNAs were synthesized using T7 Cap Scribe (Roche) according to the manufacturer's instructions. For preparation of digoxigenin labeled antisense probe, plasmid containing the usp4 cDNAs was linearized with KpnI. Linearized template DNA was transcribed *in vitro* with T7 polymerase using the digoxigenin-UTP (Roche). In situ hybridizations were performed as previously described³⁸. Embryo stages are given in Hours Post Fertilization at standard temperature (hpf).

To knockdown usp4 gene function, morpholino oligonucleotides were synthesized by Gene Tools company (zusp4-MO: 5'-

AGCGAGTGAACCCGCAGTGACCGCG-3'). Control MO sequence is 5'-GCGCCATTGCTTTGCAAGAATTG-3'. All of oligos were dissolved in nuclease-free water to make a 24 μ g/ μ l storage concentration. The mRNAs and morpholino oligonucleotides were injected into yolk of fertilized eggs at single-cell stage. All the embryo injections were carefully controlled with the same amount of control MO and control GFP mRNA.

Total RNA was isolated from embryos at different stages using Trizol reagent (TAKARA). The first strand cDNAs synthesized from total RNAs were used as templates following the SuperScript Kit (Invitrogen). qRT-PCR reactions were performed for 30 cycles and a final extension for 6 min with internal β -actin control. Primers used are list as follows:

ntl forward, 5'-ACCCTATACACCCCCACCTC-3' ntl reverse, 5'-ATAATAGGCACCGCTCATGC-3' gsc forward, 5'-GACGAGCAGCTGGAAGGCACTGGA-3' gsc reverse, 5'-TCAGCTGTCAGAATCCACGTCGCT-3' sox32 forward: 5'-ACCTTGAAATGAGACACACC-3' sox32 reverse: 5'-TGAAGGCATCTTGCTGCTCC-3' sox17 forward: 5'-CATGATGCCTGGCATGGGGGC-3' sox17 reverse: 5'-CACTCATACCTTCCGTGCAC-3'

Migration and Invasion Assays. Transwell assay were performed in 24-well PET inserts (Falcon 8.0 μ m pore size) for migration assays. MDA-MB231 stable cells were serum starved overnight. Then, 50 x 10³ or 10 x 10³ cells were plated in transwell inserts (at least 3 replicas for each sample) and left treated with or without SB431542 (5 μ M) for 8 hr. Cells in the upper part of the transwells were removed with a cotton swab; migrated cells were fixed in PFA 4% and stained with crystal Violet 0.5%. Filters were photographed and the total number of cells counted. Every experiment was repeated at least three times independently.

Zebrafish embryonic invasion and metastasis assay. We used a zebrafish embryo xenograft model developed by Snaar-Jagalska and collegues (in submission), where mammalian tumour cells are injected into the zebrafish embryonic blood

circulation. Approximately 400 tumor cells labeled with a red fluorescent cell tracer were injected into the blood of 48 hours post fertilization (hpf) *Fli-Casper* zebrafish embryos at the ducts of Cuvier³⁹ (Fig. 3d). After injection, some of the tumour cells disseminate into the embryo blood circulation whilst the rest remain in the yolk. Zebrafish embryos are maintained for 5 days post injection (dpi) at 33°C, a compromise for both the fish and cell lines⁴⁰. The tumor cells that enter into the blood stream preferentially invade and micrometastasise into the posterior tail fin area (Fig. 3e). Invasion is can be visualized as a single cell which has left the blood vessel which can subsequently form a micrometastasis (3~50 cells). Pictures were taken by confocal microscopy at 1, 3 and 5 dpi and the percentage of invasion and micrometastasis were counted. Every experiment was repeated at least two times independently.

Cellular fractions. Cytosolic, membrane and nuclear fractions were prepared using the ProteoExtract kit (Calbiochem) according to the manufacturer's instructions.

Statistical analysis. Statistical analyses were performed with a two-tailed unpaired t-test. P < 0.05 was considered statistically significant.

ACKNOWLEGEMENTS

We are grateful to Maarten van Dinther for performing the ¹²⁵I-TGF-β labeling experiment. We thank Dr. K. Iwata, Xiongbin Lu, Shengcai Lin, Stefano Piccolo and Paul Coffer for reagents. This work was supported by Netherlands Organization of Scientific Research grant (MW-NWO 918.66.606) and Centre for Biomedical Genetics.

COMPETING INTERESTS

The authors declare that they have no competing interest. Craig Mickanin, Kelly-Ann

Sheppard, Chris Lu are employed by Novartis Institutes for Biomedical Research.

REFERENCES:

- 1. Moustakas, A. & Heldin, C.H. The regulation of TGFbeta signal transduction. *Development* **136**, 3699-3714 (2009).
- 2. Kang, J.S., Liu, C. & Derynck, R. New regulatory mechanisms of TGF-beta receptor function. *Trends Cell Biol* **19**, 385-394 (2009).
- 3. Manning, B.D. & Cantley, L.C. AKT/PKB signaling: Navigating downstream. *Cell* **129**, 1261-1274 (2007).
- 4. Coffer, P.J., Jin, J. & Woodgett, J.R. Protein kinase B (c-Akt): A multifunctional mediator of phosphatidylinositol 3-kinase activation. *Biochemical Journal* **335**, 1-13 (1998).
- 5. Castaneda, C.A., Cortes-Funes, H., Gomez, H.L. & Ciruelos, E.M. The phosphatidyl inositol 3-kinase/AKT signaling pathway in breast cancer. *Cancer Metastasis Rev* 29, 751-759.
- 6. Perez-Tenorio, G., Stal, O. & Group, S.S.B.C. Activation of AKT/PKB in breast cancer predicts a worse outcome among endocrine treated patients. *British Journal of Cancer* **86**, 540-545 (2002).
- 7. Ikushima, H. & Miyazono, K. TGFbeta signalling: a complex web in cancer progression. *Nat Rev Cancer* **10**, 415-424.
- 8. Massague, J. TGFbeta in Cancer. Cell 134, 215-230 (2008).
- 9. Bakin, A.V., Tomlinson, A.K., Bhowmick, N.A., Moses, H.L. & Arteaga, C.L. Phosphatidylinositol 3-kinase function is required for transforming growth factor beta-mediated epithelial to mesenchymal transition and cell migration. *Journal of Biological Chemistry* **275**, 36803-36810 (2000).
- 10. Muraoka, R.S. *et al.* Blockade of TGF-beta inhibits mammary tumor cell viability, migration, and metastases. *Journal of Clinical Investigation* **109**, 1551-1559 (2002).
- 11. Brown, R.L. *et al.* CD44 splice isoform switching in human and mouse epithelium is essential for epithelial-mesenchymal transition and breast cancer progression. *Journal of Clinical Investigation* **121**, 1064-1074 (2011).
- 12. Zhang, Y.E. Non-Smad pathways in TGF-beta signaling. *Cell Res* **19**, 128-139 (2009).
- 13. Muraoka-Cook, R.S. *et al.* Activated type I TGFbeta receptor kinase enhances the survival of mammary epithelial cells and accelerates tumor progression. *Oncogene* **25**, 3408-3423 (2006).
- Parvani, J.G., Taylor, M.A. & Schiemann, W.P. Noncanonical TGF-beta signaling during mammary tumorigenesis. *J Mammary Gland Biol Neoplasia* 16, 127-146.
- 15. Kavsak, P. *et al.* Smad7 binds to Smurf2 to form an E3 ubiquitin ligase that targets the TGF beta receptor for degradation. *Mol Cell* **6**, 1365-1375 (2000).

- 16. Suzuki, C. *et al.* Smurf1 regulates the inhibitory activity of Smad7 by targeting Smad7 to the plasma membrane. *J Biol Chem* **277**, 39919-39925 (2002).
- 17. Nijman, S.M. *et al.* A genomic and functional inventory of deubiquitinating enzymes. *Cell* **123**, 773-786 (2005).
- 18. Yuan, J., Luo, K., Zhang, L., Cheville, J.C. & Lou, Z. USP10 regulates p53 localization and stability by deubiquitinating p53. *Cell* **140**, 384-396.
- 19. Williams, S.A. *et al.* USP1 deubiquitinates ID proteins to preserve a mesenchymal stem cell program in osteosarcoma. *Cell* **146**, 918-930.
- 20. Nakada, S. *et al.* Non-canonical inhibition of DNA damage-dependent ubiquitination by OTUB1. *Nature* **466**, 941-946.
- 21. Inui, M. *et al.* USP15 is a deubiquitylating enzyme for receptor-activated SMADs. *Nat Cell Biol* **13**, 1368-1375.
- 22. Di Guglielmo, G.M., Le Roy, C., Goodfellow, A.F. & Wrana, J.L. Distinct endocytic pathways regulate TGF-beta receptor signalling and turnover. *Nat Cell Biol* **5**, 410-421 (2003).
- 23. Zhang, X.N., Berger, F.G., Yang, J.H. & Lu, X.B. USP4 inhibits p53 through deubiquitinating and stabilizing ARF-BP1. *Embo Journal* **30**, 2177-2189 (2011).
- 24. Xu, J., Lamouille, S. & Derynck, R. TGF-beta-induced epithelial to mesenchymal transition. *Cell Res* **19**, 156-172 (2009).
- 25. Thiery, J.P., Acloque, H., Huang, R.Y. & Nieto, M.A. Epithelial-mesenchymal transitions in development and disease. *Cell* **139**, 871-890 (2009).
- 26. Kang, Y. *et al.* A multigenic program mediating breast cancer metastasis to bone. *Cancer Cell* **3**, 537-549 (2003).
- 27. Bandyopadhyay, A. *et al.* Inhibition of pulmonary and skeletal metastasis by a transforming growth factor-beta type I receptor kinase inhibitor. *Cancer Res* **66**, 6714-6721 (2006).
- 28. Tran, H., Brunet, A., Griffith, E.C. & Greenberg, M.E. The many forks in FOXO's road. *Sci STKE* **2003**, RE5 (2003).
- Wada, K. & Kamitani, T. UnpEL/Usp4 is ubiquitinated by Ro52 and deubiquitinated by itself. *Biochemical and Biophysical Research Communications* 342, 253-258 (2006).
- 30. Conery, A.R. *et al.* Akt interacts directly with Smad3 to regulate the sensitivity to TGF-beta-induced apoptosis. *Nature Cell Biology* **6**, 366-372 (2004).
- 31. Remy, I., Montmarquette, A. & Michnick, S.W. PKB/Akt modulates TGF-beta signalling through a direct interaction with Smad3. *Nature Cell Biology* **6**, 358-365 (2004).
- 32. Daly, A.C., Vizan, P. & Hill, C.S. Smad3 Protein Levels Are Modulated by Ras Activity and during the Cell Cycle to Dictate Transforming Growth Factor-beta Responses. *Journal of Biological Chemistry* **285**, 6489-6497 (2010).

- 33. Han, S.U. *et al.* Loss of the Smad3 expression increases susceptibility to tumorigenicity in human gastric cancer. *Oncogene* **23**, 1333-1341 (2004).
- 34. Cohen, P. & Tcherpakov, M. Will the Ubiquitin System Furnish as Many Drug Targets as Protein Kinases? *Cell* **143**, 686-693 (2010).
- 35. Zhang, X., Berger, F.G., Yang, J. & Lu, X. USP4 inhibits p53 through deubiquitinating and stabilizing ARF-BP1. *EMBO J* **30**, 2177-2189.
- 36. Cao, Y. *et al.* fgf17b, a novel member of Fgf family, helps patterning zebrafish embryos. *Dev Biol* **271**, 130-143 (2004).
- 37. Zhang, L. *et al.* Zebrafish Dpr2 inhibits mesoderm induction by promoting degradation of nodal receptors. *Science* **306**, 114-117 (2004).
- 38. Prince, V.E., Price, A.L. & Ho, R.K. Hox gene expression reveals regionalization along the anteroposterior axis of the zebrafish notochord. *Dev Genes Evol* **208**, 517-522 (1998).
- 39. White, R.M. *et al.* Transparent adult zebrafish as a tool for in vivo transplantation analysis. *Cell Stem Cell* **2**, 183-189 (2008).
- Lee, L.M.J., Seftor, E.A., Bonde, G., Cornell, R.A. & Hendrix, M.J.C. The fate of human malignant melanoma cells transplanted into zebrafish embryos: Assessment of migration and cell division in the absence of tumor formation. *Developmental Dynamics* 233, 1560-1570 (2005).

FIGURE LEGENDS

Figure 1 USP4 is a DUB required for TGF- β signaling. (a) Diagram of genome-wide cDNA screening data in HEK293T cells in which USPs that activate TGF-β-induced Smad3/Smad4-dependent CAGA12-Luc transcriptional reporter are indicated. The X and Y-axes are the relative luciferase activity in two replicates, p<0.01.(b,c) Effect of USP4 wild-type (USP4WT) and USP4 deubiquitin enzyme activity inactive mutant (USP4 C311S) (b) or knockdown (shUSP4 #1 and #2) (c) on CAGA₁₂-Luc transcriptional response induced by TGF- β (5 ng/ml) in HEK293T cells. Data are presented as mean \pm SD. Co.vec, empty vector; Co.sh, non-targeting shRNA. (d, e) Immunoprecipitation (IP) and immunoblotting (IB) analysis of Smad2/Smad4 complex formation in MCF10A-Ras breast epithelial cells over-expressing USP4 wt /USP4 cs mutant (d) or knocking down USP4 by shRNA (shUSP4 #1 and #2) (e) and stimulated with TGF- β (5 ng/ml) for indicated time point. (f) Kinetics of TGF- β (5 ng/ml)-induced Smad2 phosphorylation in wild type MEFs ($USP4^{+/+}$) and USP4 knock-out MEFs ($USP4^{-/-}$). Cell lysates were immunoblotted for phosphorylated Smad2 (p-Smad2) and total Smad2. (g) qRT-PCR analysis of TGF- β target genes *Smad7*, SnoN, *CTGF and PAI-1* in *USP4*^{+/+} and *USP4*^{-/-} MEFs treated with TGF- β (5 ng/ml) for indicated time points. Values and error bars represent the mean \pm SD of triplicates and are representative of at least two independent experiments. (h) The expression patterns of no tail (ntl) and goosecoid (gsc) under conditions that caused usp4 over-expression (usp4 mRNA, 100 ng) and knock-down (usp4 MO, 0.5 ng). All embryos are shown in the 70% epiboly stage. All the embryo injections

were carefully controlled with the same amount of control MO and control GFP mRNA. (i) qRT-PCR analysis of zebrafish embryos with usp4 over-expression (usp4 mRNA) or knock-down (usp4 MO). Values and error bars represent the mean \pm SD of triplicates and are representative of at least two independent experiments.

Figure 2 USP4 interacts with and deubiquitinates TBRI. (a) Endogenous TGF-B receptors of MDA-MB-231 cells were covalently affinity labeled with ¹²⁵I-labeled TGF-B ligand, cell lysates were then harvested for immunoprecipitation (IP) with TBRI, nonspecific (ns), USP4 or USP15 antibodies as indicated. Endogenous T β RI and T β RII that were immunoprecipitated by antibodies were detected by autoradiography. (b) TGF- β treatment increased the endogenous interaction between USP4 and TBRI as demonstrated by IP and immunoblotting (IB) analysis of MDA-MB-231 cells treated with TGF- β (5 ng/ml) for 4 h. Input and IP with non-specific (ns) and T β RI antibody are shown. (c) Left panel: IB analysis of whole cell lysate (TCL) and immunoprecipitates derived from HEK293T cells transfected with HA-Ub, TBRI-Flag and Myc-USP4 wt/cs and treated with or without MG132 for 2h as indicated. Right panel: the same sample from left panel was blotted with anti-Lys48-polyUb antibody. (d) HA-Ub-expressed HEK293T cells were transfected with Myc-USP4 wt/cs and treated with TGF- β (5 ng/ml) for 2 h as indicated. Cells were then harvested for IP with anti-TBRI antibody followed with IB analysis. (e) HA-Ub expressed HEK293T cells were infected with control (co.) and two independent lentivirus-mediated USP4 shRNA (#1 and #2) and treated with TGF-B (5 ng/ml) for 2 h as indicated. Left panel: cells were harvested for IP with TBRI antibody followed with IB analysis. Right panel: the sample from the left panel was blotted with

Nature Precedings : hdl:10101/npre.2012.6804.1 : Posted 19 Jan 2012

anti-Lys48-polyUb antibody. (f) Biotinylation analysis of cell surface receptors. COS7 cells transfected with caT β RI-Flag along with or without USP4 wild-type (wt)/c311s (cs) were biotinylated for 40 min at 4°C and then incubated at 37°C for various times. The biotinylated cell surface receptors were precipitated with strteptavidin beads and analyzed by anti-Flag immunoblotting. Lower right panel: quantification of the band intensities in upper panel. Band intensity was normalized to the t=0 controls. Results are shown as mean \pm SD of three independent sets of experiments. (g) MDA-MB-231 cells infected with control (Co.shRNA) or USP4 shRNA lentivirus (#1) were biotinylated for 40 min at 4° C and then incubated at 37° C with TGF- β (5 ng/ml) for indicated times to stimulate receptor internalization and treated with TGF- β (5 ng/ml) for different time point as indicated. The biotinylated cell surface receptors were precipitated with strteptavidin beads and analyzed by anti-TBRI immunoblotting. 5% whole cell lysates were loaded as input showing P-Smad2 and USP4 levels. Actin was included as a loading control. (h) Expression levels of TBRI were analysed by IB in $USP4^{+/+}$ and $USP4^{-/-}$ MEFs treated with cyclohexamide (CHX, 20 µg/ml) for the indicated time. IB for Actin was included as reference.

Figure 3 USP4 increases TGF- β -induced EMT, invasion and metastasis. (**a**) Control and USP4 stably-depleted (with shRNA #1 or #2) MCF10A-Ras cells were treated with TGF- β for 36 h and then lysed for IB analysis for changes in expression of EMT marker proteins, i.e. N-cadherin, fibronectin, smooth muscle actin (SMA), vimentin and E-cadherin. (**b**) Control and USP4 wild-type (wt)/c311s (cs) stably expressed MCF10A-Ras cells were treated with TGF- β (5 ng/ml) and SB431542 (5 μ M) for 36 h as indicated.

Cells were then harvested for IB analysis of EMT marker proteins. (c) USP4 stablydepleted MDA-MB-231 cells (#1 and #2) were plated for cell migration assays (see Methods). Cells were treated with TGF- β (5 ng/ml) for 8 h. Migrated cells were counted from four random fields, and mean \pm SD were calculated (P<0.05). Representative results are shown on the left panel. (d) Diagram of zebrafish embryonic experimental metastasis model (Methods). (e) MCF10A-Ras (M2) cells stably expressing control vector (Co.vector), USP4 WT or USP4 C311S were injected into the blood circulation of the 2 dpf zebrafish embryos. Cells were treated with or without SB431542 (10 µM) for 24 h prior to injection, and SB431542 (5 µM) was added to zebrafish environment. Pictures were taken by confocal microscopy and representative images of zebrafish at 5 days post injection (dpi) are shown. (f) Percentage of embryos displaying invasion are shown at the 1, 3 and 5 dpi. (g) The final percentage of zebrafish embryos displaying invasion and experimental metastasis at 5 dpi. The results are shown as mean \pm SD of two independent experiments. Control without SB431542 n= 144, USP4 WT without SB431542 n= 152, USP4 C311S without SB431542 n= 153, Control with SB431542 n = 152, USP4 WT with SB431542 n = 152 and USP4 C311S with SB431542 n = 153. (h) Representative light microscopy image of posterior tail of a control zebrafish embryo (upper panel) and 5 dpi zebrafish embryo displaying invasion and micrometastasis of MCF10A-Ras cells (lower panel). Red arrow indicate metastatic cells. (i) gRT-PCR analysis of TGF-β target and invasion-related genes IL-11, CXCR4, CTGF, PTHrP, MMP2 and MMP9 in MDA-MB-231 breast cancer cells infected with non-targeting shRNA or USP4 shRNA (#1) and treated with TGF- β (5 ng/ml) for indicated time point. Co.sh, non-targeting shRNA; shUSP4, USP4 shRNA. Values and error bars represent the

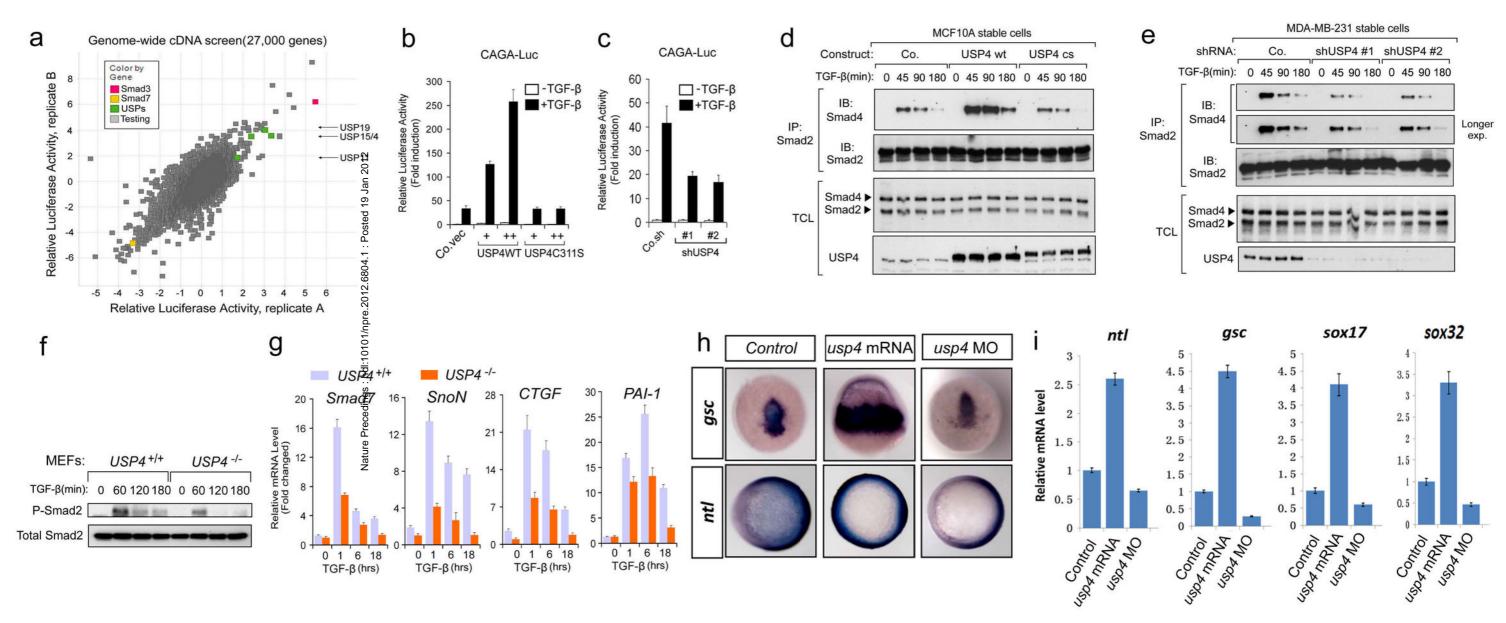
mean \pm SD of triplicates and are representative of at least two independent experiments. (j-l) MDA-MB-231 cells stably infected with empty vector (Co.shRNA) or 3 independent shRNAs (#1, #2 and #3) targeting USP4 were injected into the blood circulation of 48 hpf zebrafish. Pictures were taken by confocal microscopy and representative images of zebrafish at 5 dpi are shown (j). Invasion (k) and experimental micrometastasis (l) were detected in the posterior tail fin over 5 days. The final percentage of zebrafish embryos displaying invasion and metastasis at 5 dpi. The results are shown as mean \pm SD of two independent experiments. (p<0.05). The results are shown as mean \pm SD of two independent experiments. Control n= 175, shUSP4 #1 n= 172, shUSP4 #2 n=173, and shUSP4 #3 n= 165.

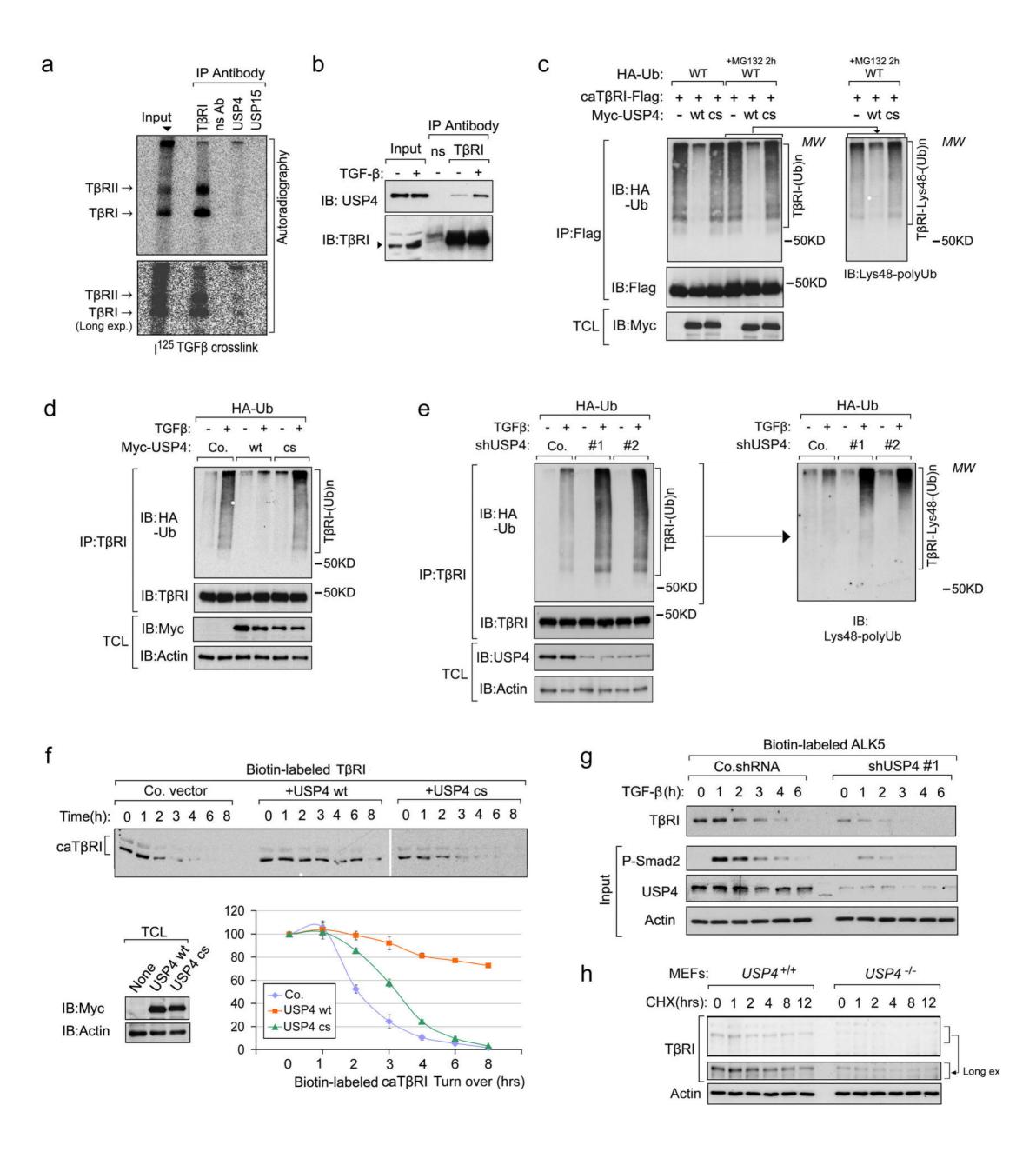
Figure 4 Akt phosphorylates USP4 and promotes its membrane and cytoplasmic localization. (**a**) Sequence alignment of Akt phosphorylation site within USP4 orthologues of different species and known Akt phosphorylating protein p27, p21 and Skp2. (**b**) Akt interacts with and phosphorylates USP4. HEK293T cells were transfected with indicated plasmids and harvest for Co-immunoprecipitation (IP) and immunoblot (IB) analysis. (**c**) Endogenous interaction between USP4 and Akt detected in HeLa cells. Cell lysates were IP with USP4 antibody followed by IB with Akt antibody. (**d**) IB analysis of whole cell lysate (TCL) and immunoprecipitates derived from HEK293T cells transfected with Flag-USP4 WT, Flag-USP4 S445A and/or HA-Myr-Akt plasmids. (**e**) IP and IB analysis of HEK293T cells transfected with Flag-USP4 S445A and/or HA-Myr-Akt and preincubated with or without λ-phosphatase as indicated. (**f**) IB analysis of whole cell lysate (TCL) and immunoprecipitates derived from serum starved

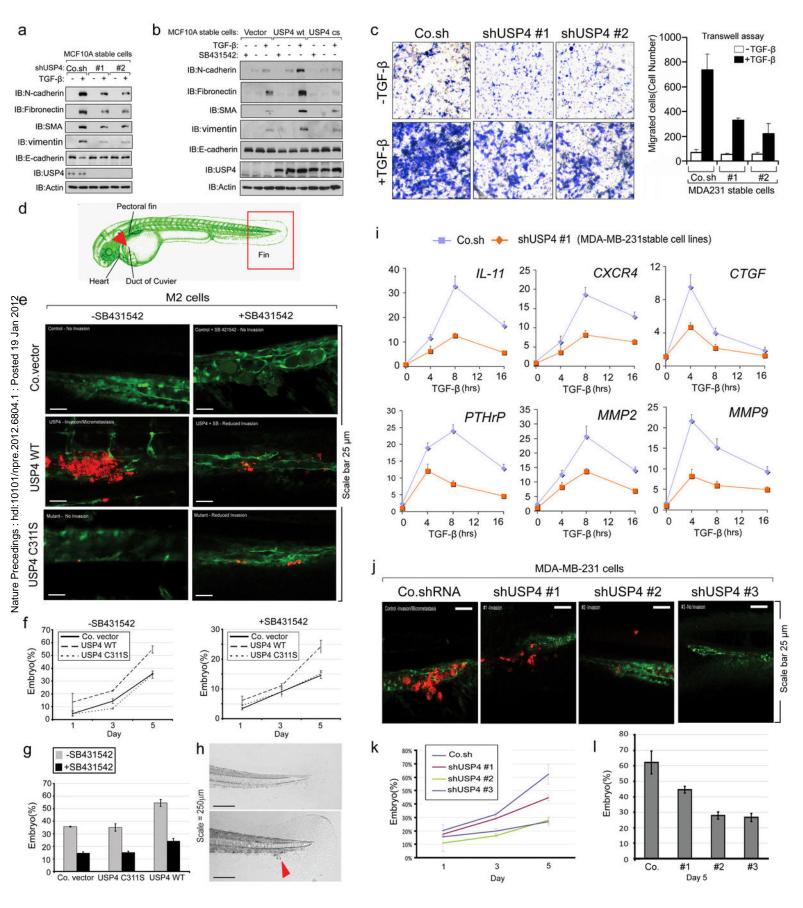
HeLa cells treated with IGF-1 (200 ng/ml), TGF- β (5 ng/ml) and LY294002 (50 μ M) for 8 h as indicated. (**g**) Immunofluorescence and 4, 6-diamidino-2-phenylindole (DAPI) staining of HeLa cells stably transfected with USP4 WT, S445A or S445D plasmids. Scale bar, 20 μ m. (**h**) Immunofluorescence and DAPI staining of HeLa cells treated with control DMSO or LY294002 (50 μ M) for 8 h. Scale bar 20 μ m. (**i**) Immunofluorescence and DAPI staining of HeLa cells transfected with HA-Myr-Akt along with USP4 WT, USP4 S445A or USP4 S445D. Scale bar, 20 μ m. (**j**) HeLa cells transfected with USP4 WT, USP4 S445A and HA-Myr-Akt as indicated were harvested for membrane, cytoplasm and nuclear extraction and followed by IB analysis. (**k**) HeLa cells were transfected with HA-Myr-Akt. 30 h after transfection, cells were treated with LY294002 (50 μ M) for 8 h as indicated. Cells were then harvested for membrane, cytoplasm and nuclear extraction and followed by IB analysis. For **j**,**k**, N-cadherin, Tubulin and HDAC3 were analysed as membrane (mem), cytoplasm (cyto) and nuclear (nuc) fraction marker, respectively.

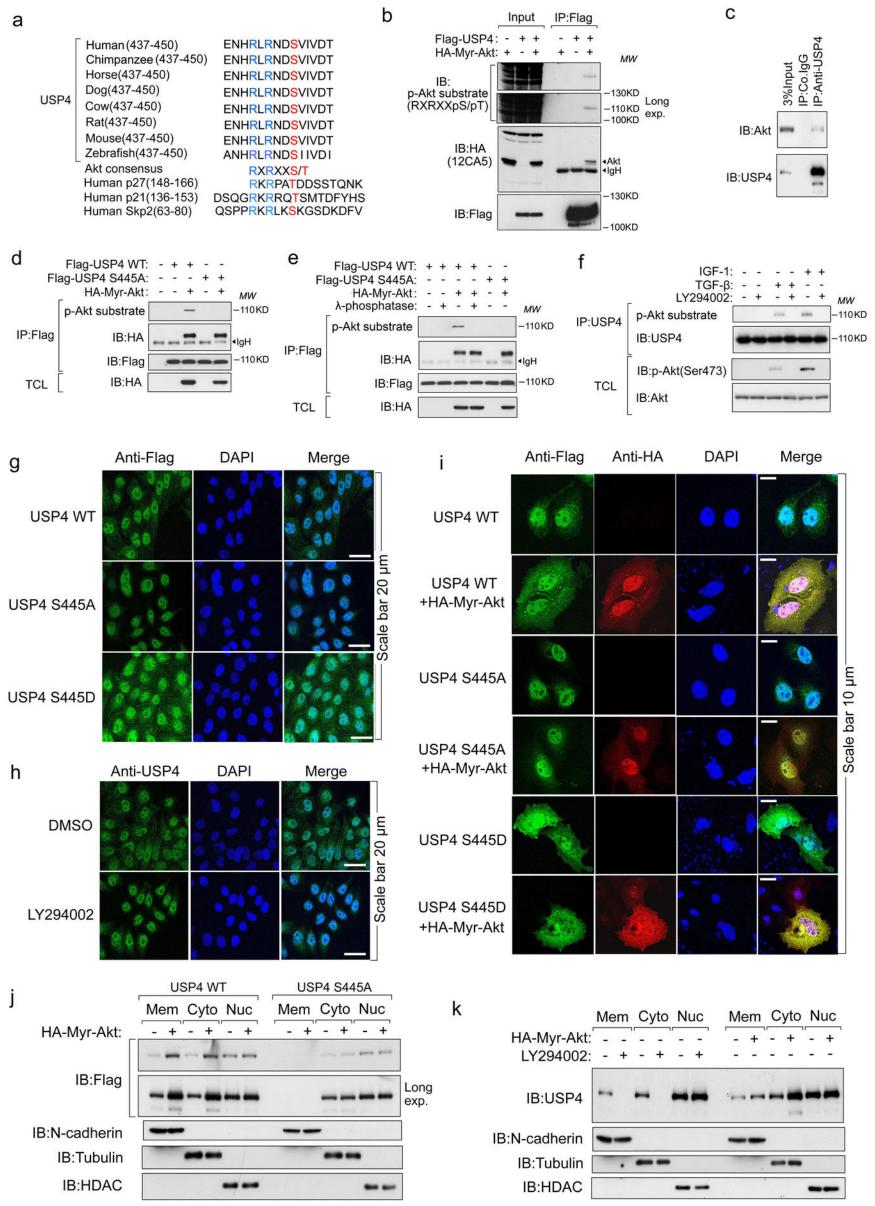
Figure 5 Akt mediated phosphorylation affects USP4 stability and DUB activity towards T β RI (**a**) Immunoblotting (IB) analysis of HeLa cells transfected with empty vector (Co.vector) or Myr-Akt and treated with DMSO, LY294002 (50 μ M) and cyclohexamide (CHX, 20 μ g/ml) as indicated. Actin was included as a loading control. (**b**)Left panel: IB analysis of HEK293T cells transfected with USP4 S445D/ USP4 S445A /USP4 WT and treated with CHX (20 μ g/ml) for indicated time point. Right panel: quantification of the band intensities in left panel. Band intensity was normalized to the t=0 controls. Results are shown as mean ± SD of three independent sets of experiments. (**c**) His-Ub stably

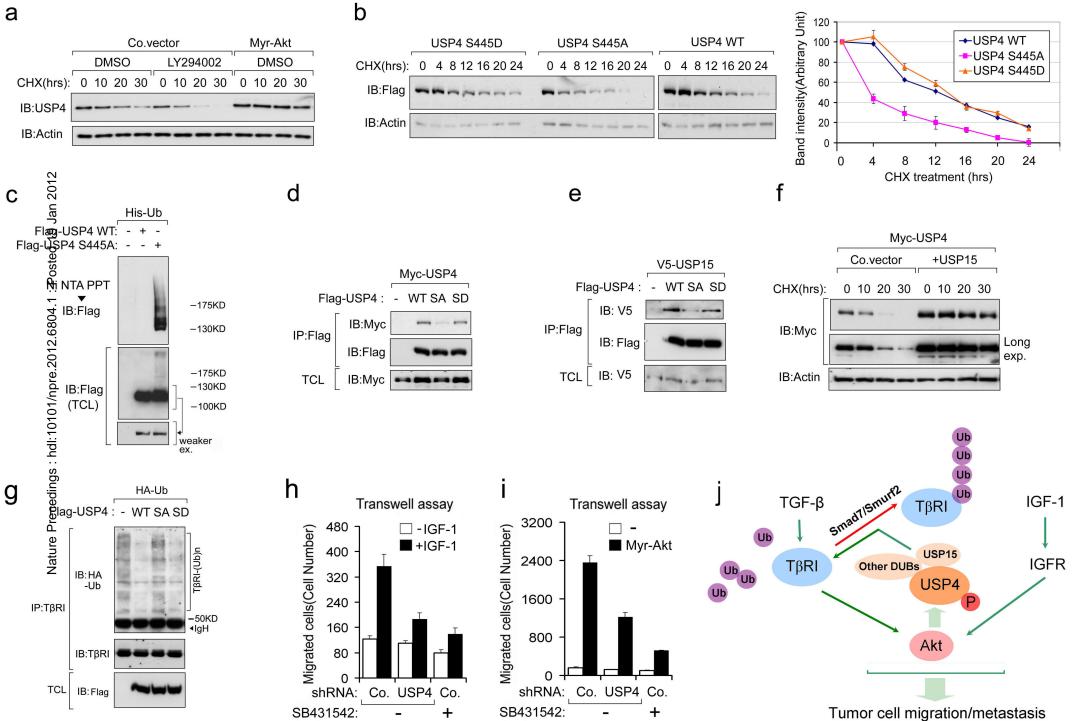
expressed HEK293T cells were transfected with Flag-USP4 WT or Flag-USP4 S445A mutant and harvested for Ni NTA pull down and IB analysis. (d,e) IB analysis of whole cell lysate (TCL) and immunoprecipitates derived from HEK293T cells transfected with Myc-USP4 (d) / V5-USP15 (e) along with Flag-USP4 WT/S445A (SA)/S445D (SD). (f) IB analysis of Myc-USP4-expressed HEK293T cells transfected with control empty vector (Co.vector) or USP15 and treated with CHX (20 µg/ml) for indicated time point. (g) IB analysis of whole cell lysate (TCL) and immunoprecipitates (IP) derived from HA-Ub-expressed HEK293T cells transfected with Flag-USP4 WT/S445A (SA)/S445D (SD). (h) Control (Co.) and USP4 stably depleted MDA-MB231 cells were plated for cell migration assays. Cells were treated with or without SB431542 (10 µM) and IGF-1 for 8 h. (i) Control (Co.) and USP4 stably-depleted MDA-MB-231 cells were infected with or without Myr-Akt and plated for cell migration assay. Cells were treated with or without SB431542 (10 μ M) for 8 h. For h and i, migrated cells were counted from four random fields, and mean \pm SD were calculated (P<0.05). (j) Working model for TGF- β signaling regulation: Akt phosphorylating USP4 serves as deubiquitinating enzyme for TBRI.











а